

# **Clean Energy Technologies**

https://ojs.ukscip.com/index.php/cet

#### **ARTICLE**

# Analysis of a Proton Exchange Membrane Fuel Cell (PEMFC) for Green Hydrogen Vehicles

Khadhraoui Ahmed 1\* 10 , Trujillo Henry 2\* 10 , Julianelli Adolfo 2 10

#### **ABSTRACT**

This work presents the development of a hydrogen-based green energy system for powering fuel cell electric vehicles (FCEVs), with a specific focus on sustainable urban transportation. Current battery-electric vehicles still face persistent challenges, primarily related to high manufacturing cost, limited driving autonomy, and the need for extensive charging infrastructure. To overcome these limitations, a novel prototype was designed and implemented, integrating an autonomous hydrogen production unit directly within the vehicle. The system is supported by photovoltaic sources for renewable energy input and Lithium-ion batteries for efficient storage and operational stability. The hydrogen produced on board is utilized by a reversible Proton Exchange Membrane Fuel Cell (PEMFC), which converts the chemical energy into electricity to drive the vehicle's engine and supply auxiliary systems. This integrated approach ensures continuous energy availability while minimizing dependence on external charging stations. The proposed concept demonstrates several advantages, including extended driving range, reduced refueling time, increased system autonomy, and zero carbon dioxide emissions. Moreover, the design contributes to urban air quality improvement and aligns with Circular Economy (CE) protocols by promoting renewable integration and

#### \*CORRESPONDING AUTHOR:

Khadhraoui Ahmed, Faculty of Science of Tunis, University of Tunis El Manar, Tunis 2092, Tunisia; Email: ahmed.khadhraoui@fst.utm.tn; Trujillo Henry, Institute on Membrane Technology, National Research Council (CNR-ITM), University of Calabria, 87036 Rende, Italy; Email: h.trujillo@itm.cnr.it

#### ARTICLE INFO

Received: 30 June 2025 | Revised: 11 August 2025 | Accepted: 14 August 2025 | Published Online: 29 August 2025 DOI: https://doi.org/10.54963/cet.v1i2.1617

#### **CITATION**

Ahmed, K., Henry, T., Adolfo, I., 2025. Analysis of a Proton Exchange Membrane Fuel Cell (PEMFC) for Green Hydrogen Vehicles. Clean Energy Technologies. 1(2): 23–40. DOI: https://doi.org/10.54963/cet.v1i2.1617

#### COPYRIGHT

Copyright © 2025 by the author(s). Published by UK Scientific Publishing Limited. This is an open access article under the Creative Commons Attribution (CC BY) license (https://creativecommons.org/licenses/by/4.0/).

<sup>&</sup>lt;sup>1</sup> Faculty of Science of Tunis, University of Tunis El Manar, Tunis 2092, Tunisia

<sup>&</sup>lt;sup>2</sup> Institute on Membrane Technology, National Research Council (CNR-ITM), University of Calabria, 87036 Rende, Italy

resource efficiency. Overall, the study highlights hydrogen-based embedded systems as a promising pathway towards clean, sustainable, and resilient mobility solutions.

Keywords: PEMFC; Green Hydrogen; Sustainable Transport; Electrochemical Modeling; Hybrid Vehicle; Simulation; FTP-75

# 1. Introduction

Most vehicles use an internal combustion engine causing significant air pollution and the inability to meet new clean energy standards for zero  $CO_2$  emissions<sup>[1]</sup>. In this context, petrol or diesel vehicles produce at least 100 grams of  $CO_2$  every kilometer, which is much higher than the Kyoto, Copenhagen recommendations and Paris COP21 policies. However, with the application of Euro 3 through Euro 6 standards, European member States must refuse to approve the registration, sale, and operation of vehicles that exceed CO2, HC and NO2 emission limits. These specifications are as follows: for Euro 3, the maximum  $CO_2$  emissions were set at 500 mg/km. However, with the implementation of Euro 6 standards in 2015, this limit was reduced to 80 mg/km. Moreover, the production of diesel cars will be phased out in Europe starting in 2030, followed by gasoline cars in 2035. **Table 1** presents the limit standard values for pollutants released in grams per kilowatt-hour (g/kWh), nitrogen oxides (NOx), carbon monoxide (CO), hydrocarbons (HC) and particles [2].

Table 1. European standards for greenhouse emissions.

Standards Reference		Date NOx (g/kWh)		HC (g/kWh)	CO (g/kWh)	
Euro 0	88/77	01-10-1990	14.4	2.4	11.2	
Euro I	91/542 (A)	1-10-1993	9	1.23	4.9	
Euro II	91/542 (B)	1-10-1990	7	1.1	4	
Euro III	1999/96	1-10-2001	5	0.66	2.1	
Euro IV	1999/96	1-10-2006	3.5	0.46	1.5	
Euro V	1999/96	1-10-2009	2	0.46	1.5	
Euro VI	Regul. (CE)	31-12-2013	0.4	0.13	1.5	

During the last decade electric vehicles (EVs) and hybrid electric vehicles (HEV), equipped with lithiumion batteries were developed and produced on a large scale to resolve this problem. For example, in 1997, Toyota launched the Prius, the first hybrid electric car to be marketed with 18,000 units, and then followed in 2010 by Nissan, Tesla, and Hyundai with 100,000 electric cars in circulation. In 2021, a Chinese electric SUV model entered the market with a price point of €40,000, featuring a 150 kW powertrain and 60 kWh battery capacity that delivered a 400 km range. The vehicle required approximately 6 hours for a full charge using a standard 6.6 kW AC charging system. However, this technology still faces significant obstacles to overcome before the internal combustion engine becomes obsolete, such as low autonomy, a slow battery charging period, as well as heavy infrastructure for installing devices and charg-

tion side, the materials required to produce batteries are very limited and may not support a true global quantity of vehicles [3].

As an alternative to the latter strategy, a second technology has recently taken hold but is not yet widely manufactured, namely green hydrogen energy technology for electric vehicles such as cars, buses, trucks, trains, and boats. Current and near future market studies estimate that the hydrogen vehicle market is taking off, especially for heavy vehicles. Hydrogen fuel cell vehicles have advantages over electric cars, such as faster times and significantly reduced battery size [4]. Without the challenges associated with hydrogen production and distribution, hydrogen fuel cell vehicles could have outperformed electric vehicles as an alternative to the traditional internal combustion engine and electric gas station charging device. As proof of this, in 2020, the Toyota Mirai sedan ing stations in kiosks or urban stations. On the produc- with an electric motor powered by compressed hydrogen

fuel cells had crossed the second generation milestone, even lower than the Hyundai Nexo. Skoda Citigo and Dacia Rabi. In 2021, a hybrid solution was proposed by PSA Automotive, which filed a patent PT/FR2022/050011, on a hybrid electric vehicle combining a hydrogen fuel cell and a Li-Ion battery, which attempted to find a technical solution for the vehicle range. But the problem of storage, whether electrical with batteries or chemical with hydrogen, remains the weak link in such an application, without forgetting security and heavy refueling infrastructure. As for public transportation, in 2017, train manufacturer Alstom launched the prototype of the Coradia train powered by hydrogen fuel cells, with support from the German Ministry of Transport. The train was launched to passengers in September 2018, with a range of 1000 km and a speed ranging from 80 Km h<sup>-1</sup> to 140 Km h<sup>-1</sup> [4]. However, hydrogen can be highly explosive, making hydrogen distribution a dangerous and expensive process<sup>[5]</sup>. To minimize this risk of explosion and to reduce the costs, this project presents the development of a new reversible fuel cell strategy to minimize hydrogen storage on the vehicle. The proposed design enables the real-time production and consumption of hydrogen through an onboard electrolysis system powered by photovoltaic panels and battery storage. This approach minimizes the need for large hydrogen storage tanks by directly feeding the generated hydrogen into the Proton Exchange Membrane Fuel Cell (PEMFC) for immediate conversion into electrical energy during vehicle operation. Such configurations have been demonstrated in experimental setups to enhance efficiency and safety while reducing system weight and complexity. Another advantage of this innovation is the increase in the vehicle energy autonomy and the minimization of the use of charging points, which facilitates the logistics and operating infrastructure of sustainable transport<sup>[5]</sup>.

This paper introduced a mathematical-empirical model of a proton exchange membrane fuel cell (PEMFC) that incorporates dynamic characteristics related to cell electrochemistry, energy balance, and reactant flow. The existing steady state model is expanded to enable dynamic electrochemical analysis <sup>[6]</sup>. The study includes electric and thermal modeling with reactant flow analysis for a well-studied fuel cell stack, specifically the Fuel

cell model<sup>[7]</sup>. Simulation of the model is performed using the Matlab-Simulink environment<sup>[8]</sup>. To validate the proposed model, a small car prototype was developed to conduct measurements and experimental results.

## 2. Materials and Methods

## 2.1. The Green Hydrogen Vehicle Structure

The primary goal of our research and innovation was to design a compact, eco-friendly vehicle powered by water. This solution aims to be both economical and sustainable by replacing compressed hydrogen with a system that generates hydrogen in real time to supply PEMFC. These fuel cells then produce the electrical energy needed to run the vehicle's engine. The process relies on water electrolysis to produce hydrogen on demand, which is used to power the fuel cell. Additionally, photovoltaic panels installed on the vehicle's roof provide supplementary energy to the battery during electrolysis, especially when the fuel cell's charge is inadequate [9].

The PEMFC fuel cell functions as an electrochemical generator, transforming chemical fuel into electrical energy. It consists of two electrodes separated by a specialized electrolyte membrane. This membrane permits the passage of ions (polarized atoms) but blocks free electrons. When fuel interacts with the anode (the first electrode) and the cathode (the second electrode) is exposed to air, a chemical reaction occurs, releasing electrons and generating an electric current [10].

The sequence of the car operating process (**Figure 1**) is as follows:

- Filling up the water tank once a month.
- The electrolyser powered by the photovoltaic panels (in the event of insufficient charge) transforms the water into hydrogen  $H_2$  and oxygen  $O_2$ .
- The O<sub>2</sub> is released into the air while the H<sub>2</sub> is recovered by the PEMFC fuel cell.
- PEMFC reacts by synthesis to reproduce water and provide an electric current cyclically and as needed.
- The DC/DC (electric converter) converts continuous electrical energy into alternating energy to operate the vehicle's electric motor.

- The car starts to drive and start according to the command from the monitor and the dashboard.
- The previous cycle operates repetitively and continuously.

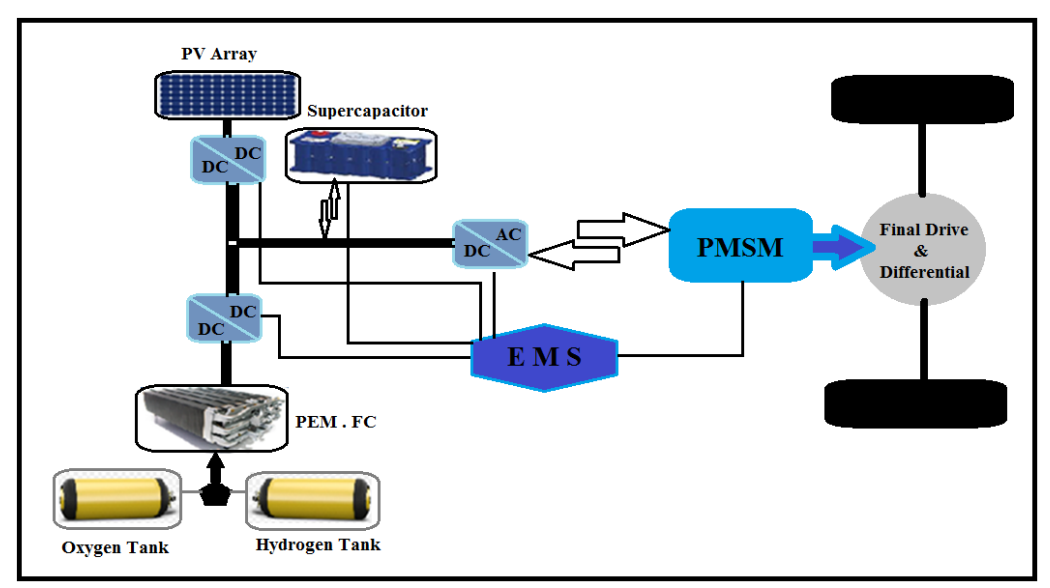


**Figure 1.** Diagram of the hybrid vehicle system, integrating onboard electrolysis, PEMFC, and photovoltaic panels for sustainable power generation.

# **2.2. Block Diagram of the Power Genera-** needed to produce hydrogen is supplied by solar PV: in the event of poor or no lighting, the battery will take over

The system is composed of three tanks: water, hydrogen and oxygen for storage to ensure a long autonomy. The fuel cell technology can operate reversibly (electrolysis and water synthesis)<sup>[11]</sup>. The electricity

needed to produce hydrogen is supplied by solar PV: in the event of poor or no lighting, the battery will take over as an auxiliary source of electricity. The battery will be recharged by braking the vehicle. The PEMFC fuel cell delivers a continuous voltage which will be converted to alternative 220V/50 Hz via an inverter (DC/AC) to fed the vehicle's AC motor (**Figure 2**).

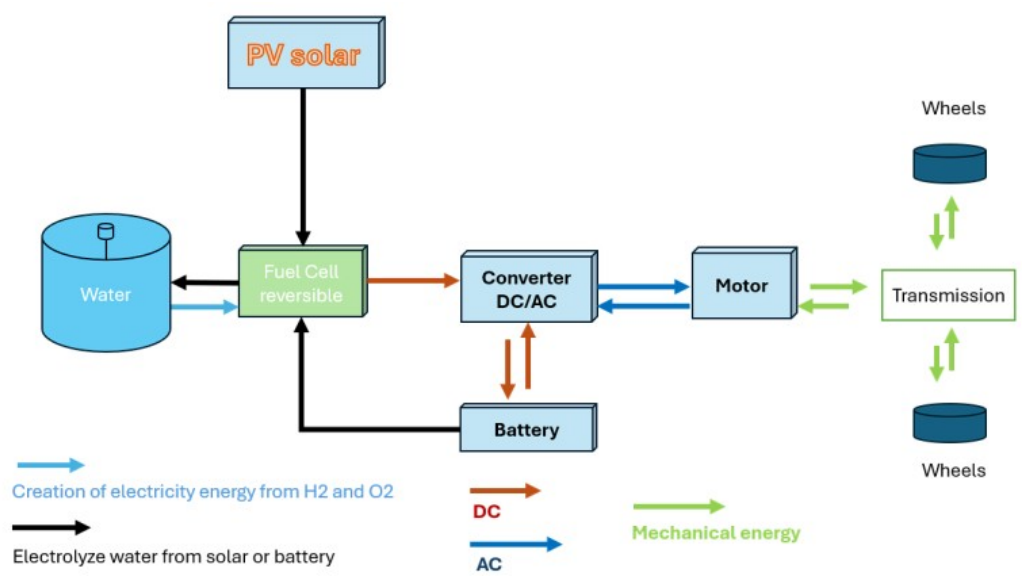


**Figure 2.** Block diagram of the electric power generation.

### 2.3. Fuel Cell System

Fuel cells are devices that electrochemically convert the chemical energy stored in a fuel, such as hydrogen, directly into electrical energy, with heat produced as a byproduct. The technology is promising for mobile and stationary applications due to its high energy efficiency in cogeneration mode, low emissions, excellent dynamic response, modularity, and durability. Among the various types under development, the Proton Exchange Membrane Fuel Cell (PEMFC) has become a leading candidate. Its advantages include a solid polymer electrolyte, rapid start-up times, a relatively low opera-

tional temperature range (50–90 °C), and a high specific energy density  $^{[11]}$ .

A typical PEMFC unit is centered around a Membrane Electrode Assembly (MEA). This core component consists of a solid polymer-ionomer membrane situated between an anode and a cathode. Each electrode is coated with a catalyst layer, often containing platinum, and a Gas Diffusion Layer (GDL). The entire assembly is compressed between conductive bipolar plates, which also feature flow channels for the reactant gases. Connecting multiple such cells in series forms a stack, enabling the system to deliver power at useful voltages and currents (**Figure 3**).

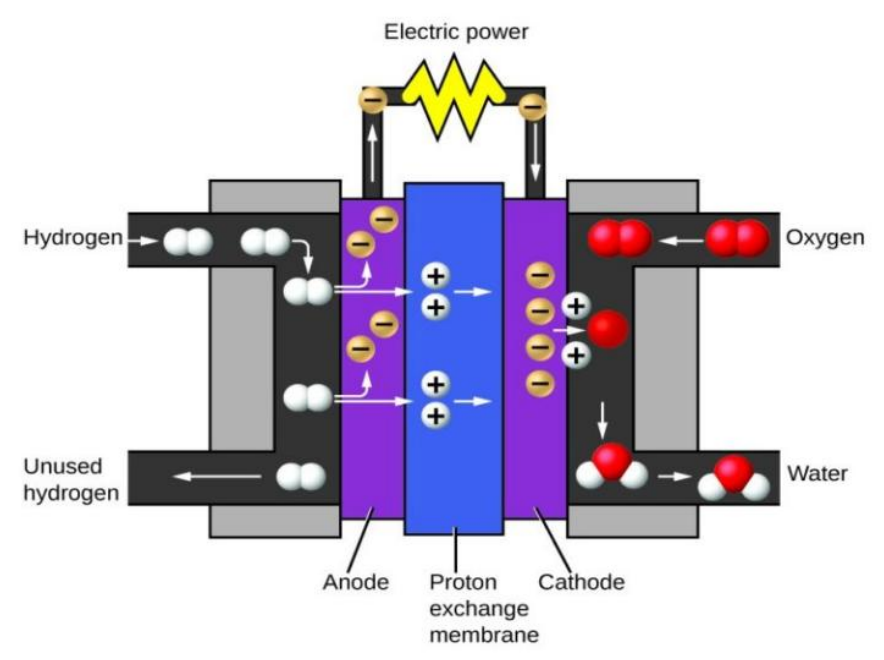


Figure 3. Fuel cell operation.

In operation, hydrogen fuel is supplied to the anode compartment, while an oxidant (typically oxygen from air) is fed to the cathode. The key electrochemical reactions occur at the three-phase boundaries within the porous electrodes. At the anode, hydrogen molecules are oxidized, releasing protons and electrons (Equation 1). The protons migrate through the ion-conductive membrane to the cathode, while the electrons travel through an external circuit, generating a useful electric current. At the cathode, oxygen molecules combine with the arriving protons and electrons to form water (Equation 2). The overall cell reaction is the combination of lows:

hydrogen and oxygen to produce water, electricity, and heat (Equation 3).

$$2H_2 \to 4H^+ + 4e^-$$
 (1)

$$4H^+ + 4e^- + O_2 \rightarrow 2H_2O$$
 (2)

$$2H_2 + O_2 \rightarrow 2H_2O + electricity + heat$$
 (3)

The operation of the PEMFC (**Figure 3**) is as follows:

- ✓ Gaseous dihydrogen (H<sub>2</sub>) coming from the tank is sent to the anode of the fuel cell, while dioxygen (O<sub>2</sub>) coming from the tank (22) arrives at the cathode.
- $\checkmark$  Molecules (H<sub>2</sub>) decompose into two protons (H<sup>+</sup>) and two electrons (e<sup>-</sup>).
- ✓ The H<sup>+</sup> ion pass through a porous membrane towards the cathode of the battery, but not the electrons which will be blocked by the membrane.
- ✓ A platinum conductive wire between the anode and the cathode allows the passage of electrons. This circulation of negative charges creates an electric current which powers the motor.
- $\checkmark$  At the cathode, H<sup>+</sup> ions and electrons combine with  $O_2$  to form water (H<sub>2</sub>O), which is released as vapor.

In addition to the main stack, a complete fuel cell system incorporates various auxiliary devices. These include a fuel processor unit, which may consist of a gas reformer, storage tank and a drive cycle of a testing vehicle. The fuel cell is considered the main source due to its ability to store large quantities of energy for an extended period. The solar panels are used for electrolysis, activated when the drive cycle is positive. In this system, dry hydrogen is supplied from a pressurized tank to the anode through a pressure regulator, maintaining anode pressure at 70 atm. A mass flow meter records the hydrogen consumption rate at the anode, while excess gas is re-circulated using a diaphragm pump. Purified air, obtained from a compressor, is supplied to the cathode, and a back pressure regulator (BPR) ensures cathode pressure remains at 3 atm (Figure 3). The fuel cell system is internally humidified, employing a circulating water stream that passes through a radiator. This process not only humidifies the reactants but also helps maintain a temperature of approximately 75 °C. The nominal stack voltage is 400 V, with a current between 100 A and 250 A. More details about the parameters of the Hydrogen Electric Vehicle (HEV) are provided in **Table 2** [12,13].

Table 2. Parameters of the HEV.

Element	Parameters	Value	
	Nominal power	90 kW	
	Number of cells (serie/parallel)	176	
Fuel Cell (PEMFC)	Hydrogen tank pressure	70 atm	
	Oxygen tank pressure	35 atm	
	Input voltage	400 V	
	MPPT power	1 kW	
PV array	Solar luminance	$1000 \text{ W m}^{-2}$	
·	Number of cells	4	
	capacity	1 kWh	
Battery	Voltage (serie/parallel)	385 V	
·	SOC	85%	
	Power	75 kW	
Vehicle	Mass	2000 Kg	
	Density	1.2 Kg m <sup>-3</sup>	

#### 2.4. The PEMFC Model

A PEMFC is not an energy storage device like a battery but an energy converter, transforming the chemical potential of hydrogen directly into electrical power via electrochemical processes. The selection of PEMFC technology for this application is motivated by its favorable attributes, which include a high power-to-weight ratio, mechanical robustness, a solid electrolyte that minimizes maintenance, rapid start-up capability, and scalability across a wide power spectrum (10 kW to 10 MW).

Furthermore, PEMFCs operate with high efficiency and produce zero greenhouse gas emissions at the point of use, aligning with environmental sustainability goals for applications ranging from centralized power generation to zero-emission transportation. The operational behavior of a PEMFC is inherently nonlinear and is governed by a multitude of interacting parameters, including operating temperature, reactant partial pressures, membrane hydration levels, and the applied electrical load. To render the system amenable to modeling and simulation, a set of simplifying assumptions is adopted [14]:

- The electrolyte membrane is assumed to be fully hydrated.
- A one-dimensional, lumped-parameter modeling approach is employed.
- The stack operates at a uniform, isothermal temperature.
- While total pressure is considered uniform, the partial pressures of the reactants are variable and impact performance.

state empirical models have been developed by Mann et al. 2000<sup>[15]</sup> and Kim et al.<sup>[6]</sup>. A generalized model outlined by Amphlett et al. [16], capable of describing various fuel cell types, is considered here, and incorporated with dynamic features to develop a basic fuel cell model. PEM

fuel cell characteristics are typically represented by polarization curves. The thermodynamic equilibrium potential of the hydrogen/oxygen reaction is reduced by various overvoltage terms associated with mass transport, and ohmic phenomena within the cell. In other words, the output voltage of a single cell is influenced by different current, temperature, and pressure-dependent factors.

### For the electrochemical modeling, several steady- 2.5. Equivalent Diagram of a Fuel Cell

The electronic model of the fuel cell can be illustrated by the diagram of Figure 4. The model is equivalent to a Thevenin generator characterized by its couple (Enernst,  $R_{th}$ ) which delivers on an electrical load <sup>[17]</sup>.

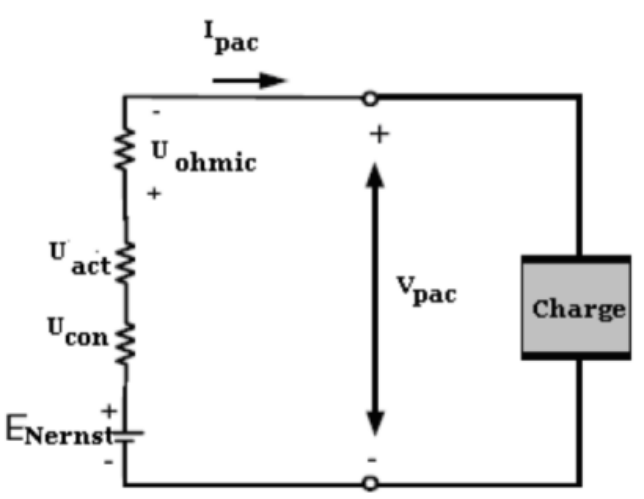


Figure 4. Electric model of a fuel cell.

The  $R_{th}$  is the internal resistance of Thevenin gen- as follows [18]: erator, and can be expressed as:

$$R_{th} = R_{com} + \frac{R_{act} + R_{com}}{1 + jCw(R_{act} + R_{com})}$$
 (4)

 $w = 2\pi F$ 

F: frequency

As the current in the fuel cell is continuous, we can adopt F = 0.

In this case,  $(R_{th})$  becomes:

$$R_{th} = R_{act} + R_{ohm} + R_{com} \tag{5}$$

The output voltage of the fuel cell can be expressed

$$E_{FC} = E_{nernst} - V_{act} - V_{ohm} - V_{com}$$
 (6)

The expression of the Nernst equation [19] is as follows [20]:

$$E_{Nernst} = 1.229 - 0.85 * T^{-3}(T - 298.15) + 4.3085 * 10^{-5}T \left[ \ln \left( P_{H_2} \right) + 0.5 * \ln \left( P_{O_2} \right) \right]$$
(7)

 $P_{H_2}$  and  $P_{O_2}$  are respectively the pressures of hydrogen and oxygen at the inlet of the cell expressed in atmospheres (atm). According to Amphlett's model and the following [21]:

$$V_{act} = [\xi_1 + \xi_2 T + \xi_3 T \ln(C_{O_2}) + \xi_4 T \ln(I_{FC})]$$
 (8)

With

 $I_{FC}$  is fuel cell current.

 $\xi_1, \xi_2, \xi_3$  and  $\xi_4$  are parameters of the fuel cell.  $C_{o2}$  is the concentration of Oxygen (mol cm<sup>-3</sup>).

 $C_{o2}$  can be computed by Henry expression as follows<sup>[22]</sup>.

$$C_{o2} = \frac{P_{o2}}{5.08 * 10^6 e^{-498/T}} \tag{9}$$

The ohmic drop voltage across the cell is the result of the electronic resistances of the bipolar plates and can be given by the expression<sup>[19]</sup>:

$$V_{ohm} = I_{FC}(R_M + R_C) \tag{10}$$

Where

$$R_M = \xi_5 + \xi_6 T + \xi_7 I_{FC} \tag{11}$$

- $R_M$ : is the resistance of the membrane.
- R<sub>C</sub> is the contact resistance to the conduction of electrons.

The concentration voltage is the following [23]:

$$V_{com} = B\left(\frac{J}{Jmax} - 1\right) \tag{12}$$

Finally, the output voltage of the PEMFC is:

$$V_{stack} = N_{cell} * E_{FC} \tag{13}$$

- $V_{stack}$  is the output voltage of the PEMFC (all cells).
- $N_{cell}$ : number of cells in series.
- $E_{Nernst}$ : is the thermodynamic. potential of a single cell Vact: is the activation voltage.
- $V_{ohm}$ : is the ohmic voltage.
- $V_{com}$ : is the concentration voltage
- T: cell temperature (K).
- $PH_2$ : Hydrogen pressure (atm).
- $P_{02}$ : Oxygen pressure (atm).
- J: is the current density of the cell (A cm<sup>-2</sup>).
- $J_{max}$ : is the maximum current density of the battery (A cm<sup>-2</sup>).
- *B*: is a weighting constant.

The values of the used parameters of the PEMFC are presented in **Table 3**.

**Table 3.** Parameters values [20].

Parameter	Value	Parameter	Value
$\xi_1$	$-6.5 \times 10^{-1}$	ξ5	3.3
$\xi_2$	$4.3 \times 10^{-3}$	$\xi_6$	$-7.5 \times 10^{-3}$
$\dot{\xi}_3$	$-1.9 \times 10^{-4}$	ξ7	$1.1 \times 10^{-3}$
$\xi_4$	$1.8 \times 10^{-5}$	$J_{m{max}}$	0.05
R.C.	$3 \times 10^{-3}$	$P_{H2}$	0.1
В	$16 \times 10^{-3}$	$P_{O2}$	0.1

### 2.6. The Vehicle Modeling

Electric vehicles are subject to physical forces during driving, such as gravity, wind, rolling resistance, and inertial force that affect vehicle motion. The driving force required by the vehicle can be calculated by the following expression<sup>[24]</sup>:

$$PL = PR + PAR + PA + PG \tag{14}$$

Where:

- PL: is driving force.
- *PR*: is the rolling resistance.

- *PAR*: is the wind force.
- *PA*: is the inertia force.
- *PG*: is the gravity vehicle force.

$$PL = C_R M_{hev} * g * cos(\alpha)$$
 (15)

$$PAR = 0.5 * \rho.C_{AR} * A_V * V_{hev}^2$$
 (16)

$$PA = M_{hev} * A_{hev} * V_{hev} \tag{17}$$

$$PG = M_{hev} * q \sin(\alpha) \tag{18}$$

#### With:

- $C_R$ : is the vehicle coefficient of rolling resistance.
- $M_{hev}$ : is the vehicle mass (2000).
- $V_{hev}$ : is the vehicle speed (km h<sup>-1</sup>).
- $A_{hev}$ : is the vehicle acceleration (m s<sup>-2</sup>).
- $A_V$ : is the vehicle equivalent cross-section (m<sup>-2</sup>).
- g: the gravity (9.81 m/s $^2$ ).
- $\rho$ : Air density (kg m<sup>-3</sup>).
- $\alpha$ : is the street inclination.

The required vehicle power can be expressed as:

$$P_{REQ} = \frac{P_{EV} - P_{BK}}{\eta_{GX} * \eta_{inv} * \eta_M} \tag{19}$$

#### Where:

- $P_{EV}$ : is the electric vehicle power.
- $P_{BK}$ : is the braking power.

- $\eta_{GX}$ : is the gear efficiency.
- $\eta_{inv}$ : is the inverter efficiency.
- $\eta_M$ : is the vehicle motor efficiency.

# 3. Simulation Results

#### 3.1. PEMFC Simulation

The non-ideal voltage losses—activation, ohmic, and concentration significantly influence the operational efficiency of the PEMFC, as documented in prior studies<sup>[25-27]</sup>. **Figure 5** presents a simulated polarization curve, which exhibits three distinct regions: a sharp initial voltage drop at low currents due to activation polarization, a linear decline in the mid-current range dominated by ohmic losses, and a rapid voltage fall-off at high currents caused by mass transport limitations.

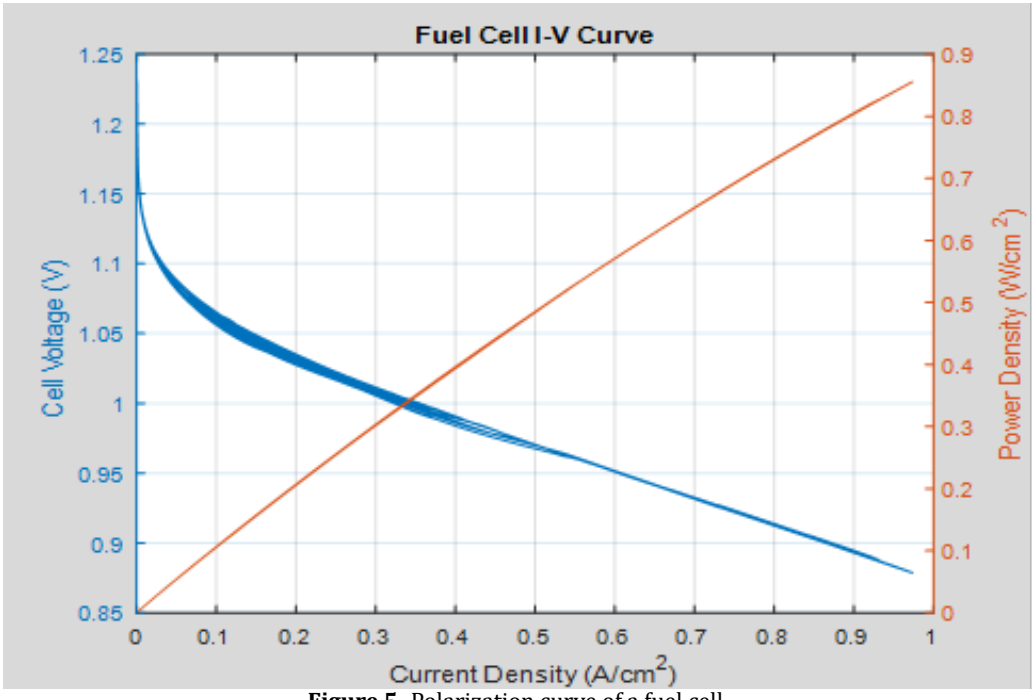


Figure 5. Polarization curve of a fuel cell.

The developed dynamic model was implemented in the Matlab-Simulink environment (Figure 6). The simulation incorporates the PEMFC stack model integrated with its auxiliary systems, including reactant supply and a defined drive cycle. The model inputs are the controlled flows of pressurized hydrogen and air. The stack's output voltage is dynamically computed based on the load current, operating temperature, and reactant pressures. The simulation period, set to 2500 seconds, was chosen to capture the system's complete transient response under the specified driving profile, as shown in Figure 7.

The parameters of the fuel sale are set in **Table 4**.

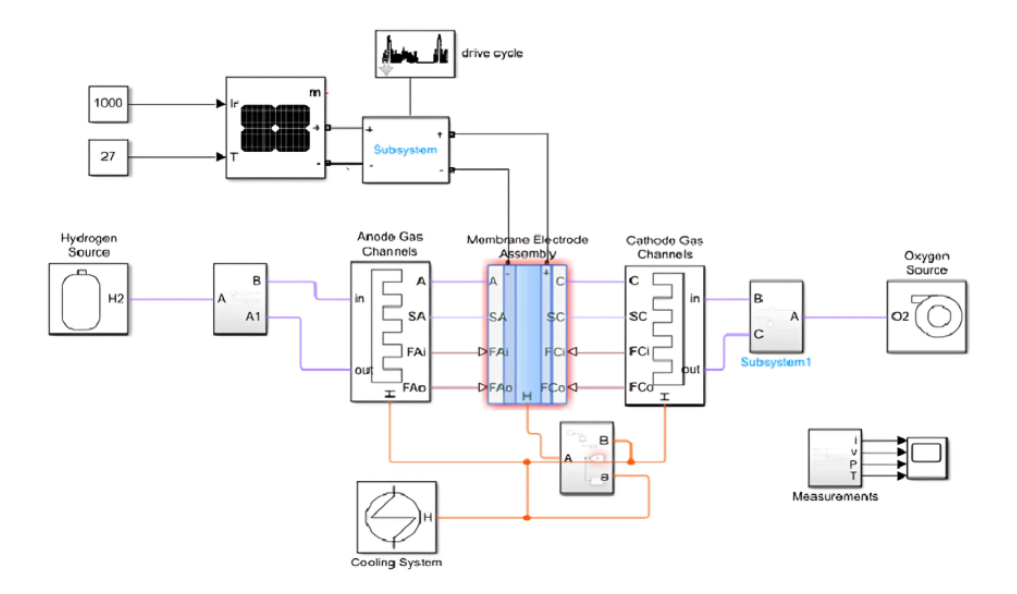
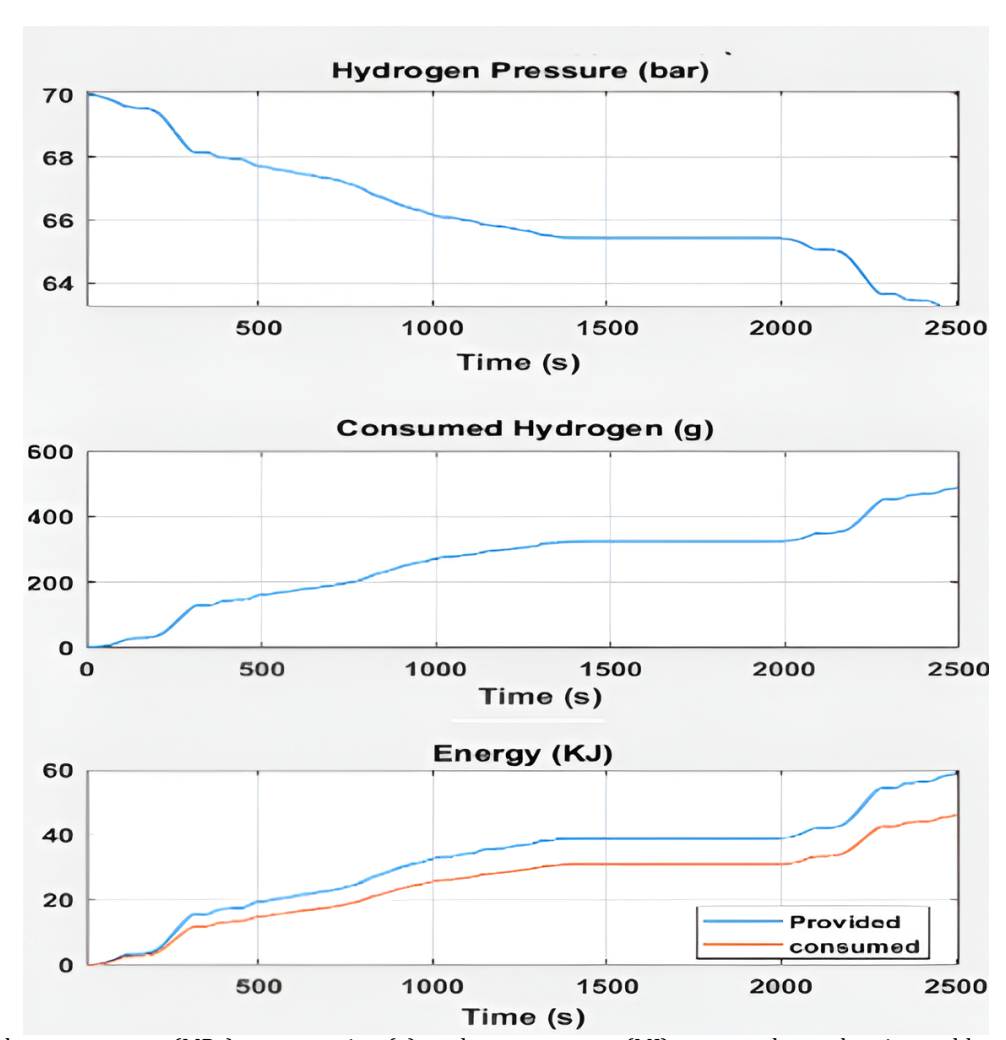


Figure 6. Fuel cell system Simscape model.



**Figure 7.** Hydrogen pressure (MPa), consumption (g), and energy output (MJ) over one hour, showing stable operation at 63 MPa after consuming  $500 \text{ g H}_2$ .

Parameter	Value	Name		
N <sub>cell</sub>	400	Number of cells in stack		
area <sub>cell</sub>	$280 \text{ cm}^{-2}$	Cell area		
$t_{membrane}$	125 μm	Membrane thickness		
$t_{gdl_A}$	250 μm	Anode gas diffusion layer (GDL) thickness		
$t_{gdl_C}$	250 μm	Cathode gas diffusion layer (GDL) thickness		
$i_o$	8e-05 A cm <sup>-2</sup>	Exchange current density		
$i_L$	1.4 A cm <sup>-2</sup>	Max (limiting) current density		
$\alpha$	0.5	Charge transfer coefficient		
$ ho_{membrane}$	$2000~{ m Kg}~{ m m}^{-3}$ Density of dry membrane			
$M_{membrane}$	$M_{membrane}$ 1.1 Kg mol <sup>-1</sup> Equivalent weight of dry membrane			

# **3.2. Consumed Hydrogen, Produced En-** the storage tank is 5 kg of H<sub>2</sub>, then the PEMFC autonomy ergy and Autonomy

The amount of hydrogen needed to power a 90 kW fuel cell (PEMFC) is:

$$H_{cons} = P_{FC} * \eta * D_H \tag{20}$$

- $P_{FC}$ : is the energy density of hydrogen = 33 kWh/kg
- $\eta$ : is the efficiency of the PEMFC cell = 55%
- $D_H$ : is the power of the PEMFC = 90 kW

These values give hydrogen consumption around 1.36 kg/h. The autonomy of the vehicle in hours, can be deduced as:

$$A_{H(in\ Hours)} = V_{st}/H_{cons} \tag{21}$$

 $V_{st}$ : is the volume of the storage  $H_2$  tank.

If we adopt a speed ( $S_p$ : in km/h), then the autonomy in kilometers will be:

$$A_{k(in\ km)} = S_p * A_H \tag{22}$$

In the case where the mean speed is 80 km/h and

is equal to 3.67 hours or in other terms around 300 km.

Figure 7 gives an illustration of the hydrogen pressure, consumption and provided energy during the first hour of driving or functioning. We can observe that the fuel cell is under 70 bar pressure (Figure 7). However after 2500 sec, it becomes 63 (MPa) and this occurs after the consummation of 500 (g) of hydrogen which develops an energy of 44 MJ or an equivalent of 12 kWh.

# 4. Vehicle Test Procedure

The Federal Test Procedure (FTP)-75 test procedure for the city vehicle driving cycle is a series of standard tests defined by the United States Environmental Protection Agency (EPA) to measure exhaust emissions and fuel consumption of gasoline-diesel, electric and hybrid cars, and also to estimate the range in distance traveled by an electric vehicle.

The test protocol which is illustrated in the **Figure 8**, is divided into four phases. The characteristics of the cycle are as follows: - Distance traveled: 17.7 km - Duration: 1874 seconds - Average speed: 34 km/h.

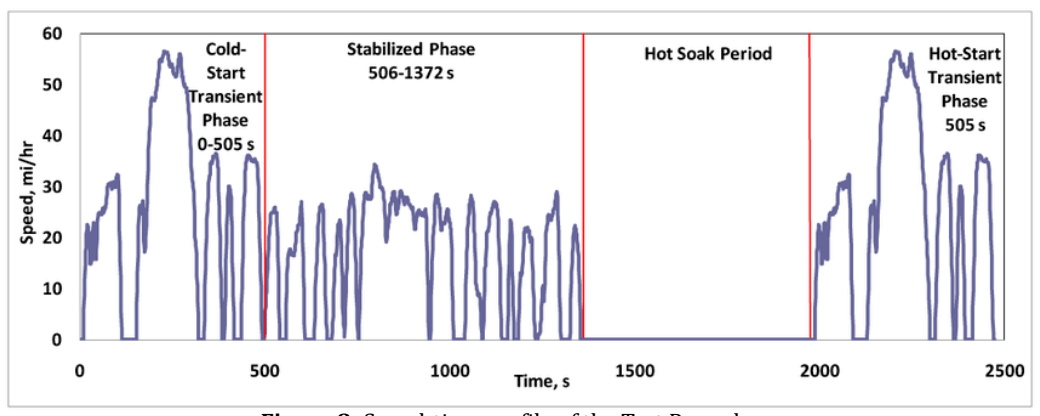


Figure 8. Speed-time profile of the Test Procedure.

According to **Figure 9**, we can observe the temporal evolution of PEMC current, voltage, power and temperature during the first hour according to FTP-75 test protocol. We can observe a concordance of the vehicle behavior with the target profiles of **Figure 8**. Cold and hot starting periods are zones where the consumed hydrogen and power are highest (80KW), how-

ever the temperature of the fuel cell is maintained stable around 80 degree during the cycle of the functioning. The contribution of the oxygen is to reduce the cell temperature, which we observe in the third zone (1400–2000 sec): in this case, the temperature of the cell began to decrease gradually, reaching 70 degree at 2000 sec.

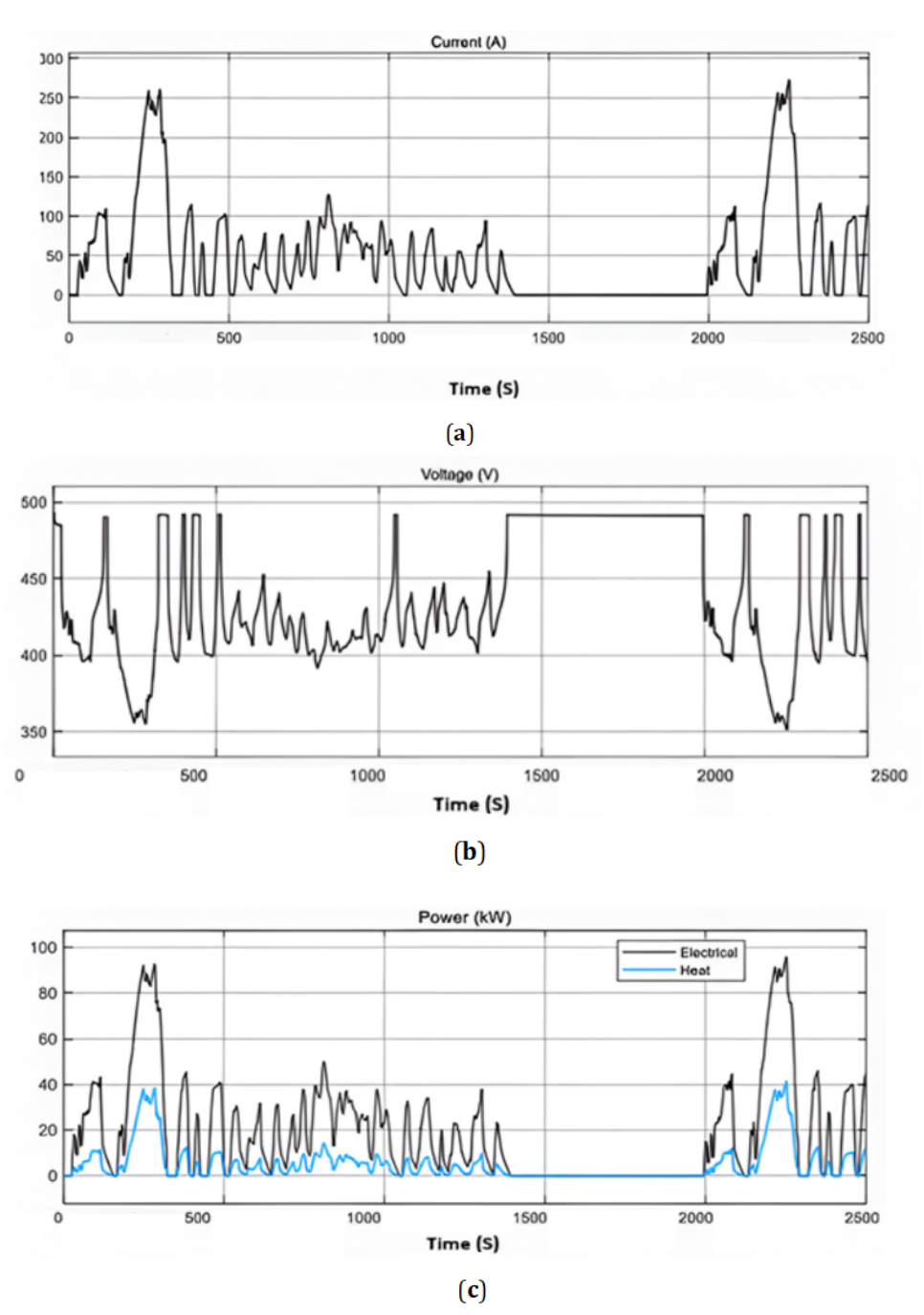
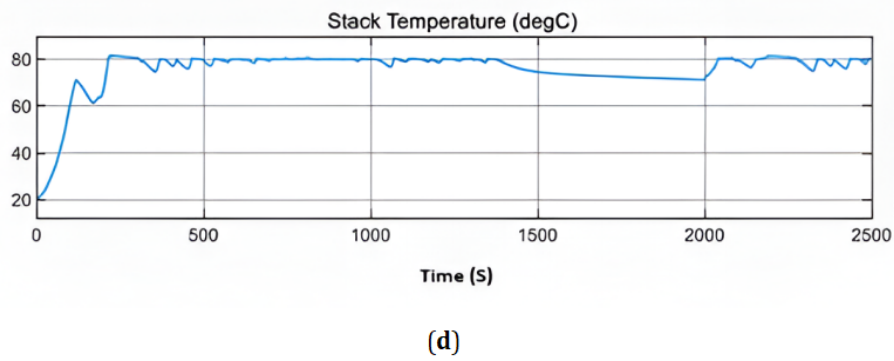


Figure 9. Cont.



**Figure 9.** PEMFC current (A) (a), voltage (V) (b), power (kW) (c), and temperature (°C) (d) during FTP-75 test, showing stable operation and cooling effect of oxygen flow.

# 5. Vehicle Speed

The FTP-75 speed profile and protocol was used and the time was set to 1400 seconds which correspond to first and second periods of the protocol (starting or transit period, stable or permanent period). **Figure 10** 

represents the temporal speed profile of the HEV during the 1400 seconds. In comparison with the standard FTP-75 profile, the vehicle traveled almost 18 km at a speed above 37 km/h and reaches its stable regime at full energy from 200 seconds (**Figure 10**).

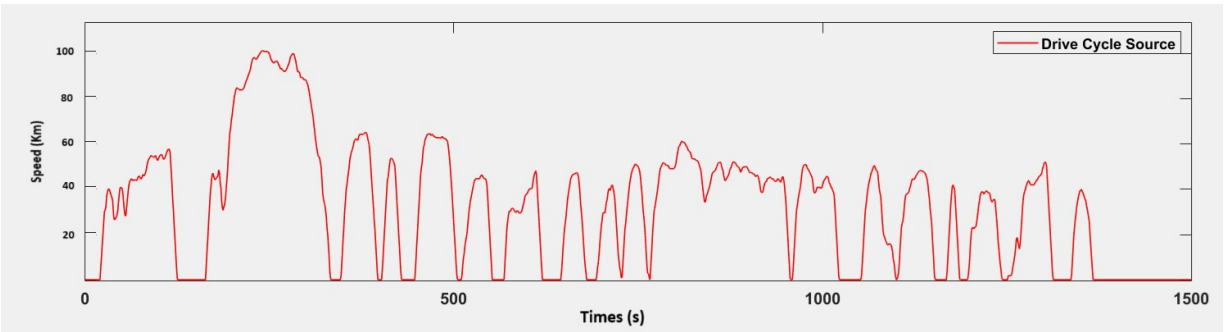
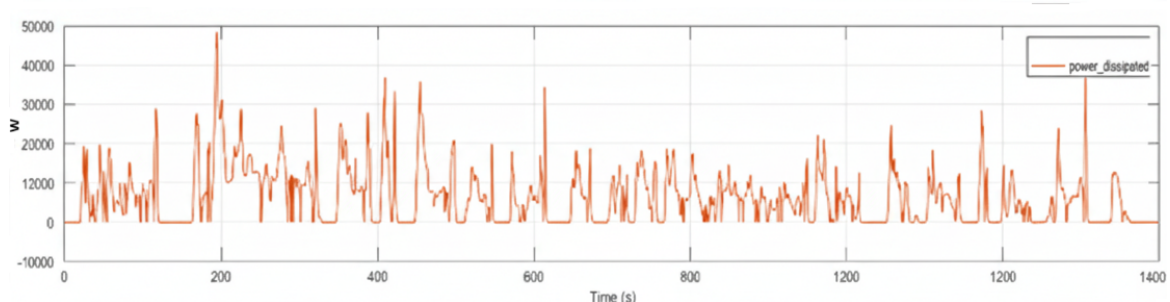


Figure 10. Temporal speed profile of the HEV.

Up to 505 seconds, the vehicle went through its cold start transient period characterized by significant vibration before reaching its highest speed. Then the cycle was stable up to 1372 seconds at intermediate speed. Finally, the vehicle speed returned to zero for the remainder of the cycle (1400 seconds). The maximum produced power, P = 45 kW, for a maximum of 170 seconds. The obtained results demonstrate the hybridization benefit of the PEMFC fuel cell and the battery to give more efficiency and power to the electric vehicle motor.

**Figure 11** shows the evolution of the vehicle's supplied power during the same period of 1400 seconds. Shows that at the beginning of the cycle, current is fully

drawn from the battery, then current is drawn from the PEMFC for the rest of the cycle. We can notice that during any braking, the fuel cell remains on standby and the battery goes to the recharge phase, although the braking time is the braking delay. It is a common practice that the PEMFC is slower in terms of operating response and that is why the battery is supposed to start powering the electric motor. The battery terminal voltage varies according to vehicle operation conditions. Furthermore, the battery state of charge (SOC) varies between 48.5% and 60% as illustrated in **Figure 12**. The obtained results demonstrate the hybridization benefit of the PEMFC fuel cell with Li-Ion battery to give more efficiency and power to the electric vehicle motor.



**Figure 11.** Provided vehicle power.

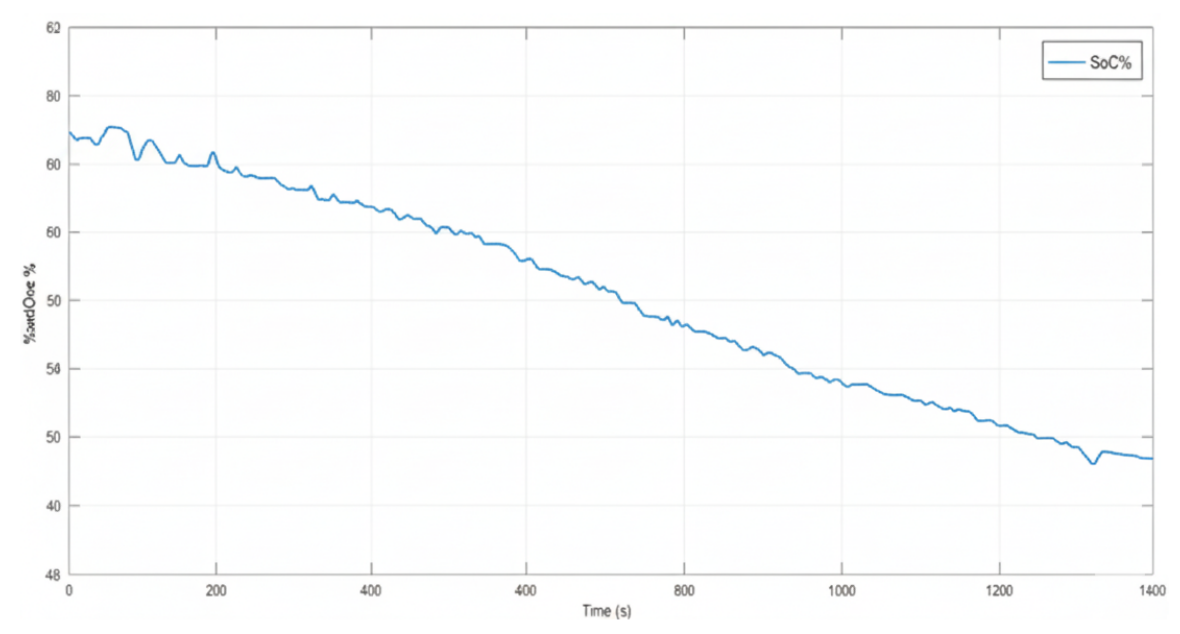


Figure 12. Battery State of Charge during the cycle FTP75.

# 6. Discussion

The reversible PEMFC coupled with a hydrogen tank and the vehicle's battery forms a more powerful hybrid propulsion system. When the vehicle is moving, the PEMFC produces electricity from hydrogen to power the electric motor. When the vehicle is stationary, the PEMFC can operate in electrolyzer mode to recharge the battery from water, using electricity from solar panels. This hybridization between battery-electric cars and hydrogen-powered cars is highly advantageous from a propulsion and power perspective. The electric battery provides good energy efficiency for urban journeys, while the hydrogen fuel cell ensures greater autonomy, shorter recharge times, and suitability for longer trips. Additionally, this hybridization reduces the weight and size of the electric vehicle by de-

creasing battery volume. It also offers more flexibility for the driver, who can choose the appropriate combination of battery and/or fuel cell usage depending on their journey and needs, optimizing energy efficiency based on driving conditions.

The hybrid PEMFC-battery system enhances propulsion efficiency, with the PEMFC providing steady power and the battery handling peak demands. Experimental validation on the prototype yielded voltage-current curves (400–500 V, 100–250 A), an efficiency of 55%, and a hydrogen output of 1.36 kg/h, aligning with simulation results. The 5 kg  $\rm H_2$  tank (70 atm) supports dynamic driving conditions, with onboard electrolysis producing approximately 0.5 kg/h  $\rm H_2$ , supplemented by the tank during sudden power demands (e.g., acceleration). Excess hydrogen is stored, ensuring no shortages during FTP-75 cycles. This approach minimizes the need for large hydro-

gen storage tanks, enhancing safety and reducing system weight.

Modeling Limitations: The isothermal and constant-pressure assumptions simplify the model but may overestimate efficiency by 5--10% under variable conditions, such as rapid temperature changes or pressure drops. Future models could incorporate transient thermal dynamics and pressure fluctuations to improve accuracy and better reflect real-world performance.

The obtained results demonstrate that the performance of a fuel cell is highly dependent on the temperature of the stack. Higher temperatures typically elevate the polarization curve, indicating enhanced performance. However, excessively high temperatures can lead to membrane dehydration and stack degradation. Therefore, maintaining an optimal temperature (between 70 and 80 °C) is crucial for achieving peak performance. The effective partial pressure of hydrogen and oxygen in the fuel cell is determined by the reactant flow rates at the anode and cathode, as well as the magnitude of the stack current. Analytically, an increase in fuel cell current corresponds to a higher consumption of hydrogen and oxygen, leading to a decrease in reactant pressure.

The fuel cell stack is projected to generate a maximum power of 90 kW at an operating temperature of approximately 80 °C. The voltage input for the PEMFC falls within the range of 400 to 500 V. A slow chemical reaction in the activation region leads to a nonlinear voltage drop due to a reduction in voltage. Following the activation region, the fuel cell operates in the ohmic region, with a voltage drop from about  $475 \, \text{V}$  to  $415 \, \text{V}$ . The ohmic loss in this region is caused by electrical resistance in the electrode, resulting in a linear voltage drop. The region

of maximum performance, at 205 A and 440 V, is considered ideal for fuel cell operation. Transitioning from the ohmic region, the fuel cell enters the mass transport region, starting at around 415 V and ending near 400 V. The loss of mass concentration in this region is due to the diffusion of reactants from flow channels to reaction sites, with slower transportation of reactants in higher current operating regions leading to a more noticeable loss.

On the other hand, the tests of the hydrogen electric vehicle according to the FTP-75 protocol showed that the speed of the car reached its steady state with the desired values after 200 seconds. However, the power provided by the fuel cell is 45 kW for reduced speeds not exceeding 50 km/h. The deficit is provided by the battery, especially during acceleration or high speeds. The values obtained showed that the average hydrogen consumption is approximately 0.5 kg/100 km, which provides an energy output of 15 kWh and a range of 4 hours or approximately 300 km for an average speed of 80 km/h. These values are encouraging, especially since they can be improved if an energy and driving management supervisor is used.

By comparing our results with those from other references and international organizations, as well as recent HEV developments by Toyota, Hyundai, BMW, Honda, and Mercedes, indicators show that our model is competitive despite being a non-industrial prototype in the final stages of development. Observing the values in **Table 5**, we notice that our HEV model performs comparably to other hydrogen vehicles. If we double the power of our prototype, we could match the performance of BMW and Hyundai models while potentially exceeding them in efficiency.

**Table 5.** Performances indicator's Comparison with recent HEV models [28].

Model	Power (KW)	Autonomy (km)	H <sub>2</sub> Tank (kg)	Time of Charging (min)	Consumption (kg) $H_2/100 \text{ km}$	Vehicle Mass (kg)
Toyota Mirai	114	650	5.6	3-5	0.76	1850
Hyundai Nexo	120	666	6.3	5	0.95	1950
Honda Clanty	130	589	5.5	3-5	0.84	1830
BMW I Hydrogen	170	500	6.0	3-4	1.20	2100
Mercedes-Benz	147	493	4.4	3	1.03	2345
Hyundai XCIENT	190	400	32.0	8-20	1.50	19500
Our model	90	300	4	5	0.5	2000

# 7. Conclusions

The transition towards sustainable urban transportation has been a pivotal focus in recent years, driven by the imperative to reduce carbon emissions and air pollution. (EVs) and (HEVs) equipped with lithium-ion batteries have emerged as promising alternatives to traditional internal combustion engine vehicles. However, despite their potential, EVs and HEVs face significant challenges, including limited range, prolonged charging times, and the need for extensive charging infrastructure. In response to these challenges, a novel approach utilizing hydrogen-based green energy for powering electric vehicles has been proposed and developed in this study.

By integrating an on-board hydrogen production system with a photovoltaic source and Li-Ion battery, the proposed system extends vehicle range, boosts motor propulsion, reduces recharge times and offers more energy flexibility during driving.

The developed car prototype is designed with regenerative braking and energy recovery, in no-load, deceleration or braking mode. The drive is done without a gearbox and without drive shafts, resulting in a reduction in the weight of the vehicle, the bulk and the power required. The analysis study is based on both empirical and fundamental physical relationships, capturing various aspects related to transient phenomena in cell electrochemistry, energy balance, and reactant flow. The models are simulated using Matlab-Simscape software, and then compared with experimental data, collected from a small prototype developed in our laboratory. The obtained results demonstrated that the fuel cell (FC) could provide approximately 70% of the required current once the vehicle was in motion, with the remaining 30% supplied by the battery.

Finally, the scalability of hydrogen fuel cell technology presents opportunities for applications beyond passenger vehicles, including buses, trucks, trains, and boats. This versatility positions hydrogen as a viable solution for a wide range of transportation needs. Despite the promising prospects of hydrogen-based green energy systems, several challenges must be addressed such as the high cost and the security structure of hydrogen storage which requires high safety devices.

# **Author Contributions**

Conceptualization, K.A., T.H., and I.A.; methodology, K.A., T.H., and I.A.; software, K.A., T.H., and I.A.; validation, K.A., T.H., and I.A.; formal analysis, K.A., T.H., and I.A.; investigation, K.A., T.H., and I.A.; resources, K.A., T.H., and I.A.; data curation, K.A., T.H., and I.A.; writing—original draft preparation, K.A., T.H., and I.A.; writing—review and editing, K.A., T.H., and I.A.; visualization, K.A., T.H., and I.A.; project administration, K.A., T.H., and I.A.; All authors have read and agreed to the published version of the manuscript.

# **Funding**

This research received no external funding.

# **Institutional Review Board Statement**

Not applicable.

# **Informed Consent Statement**

Not applicable.

# **Data Availability Statement**

The data presented in this study were generated from simulations performed in our laboratory using Matlab software. No new raw data were created or analyzed that are not already included in the figures and tables of this article.

# **Conflicts of Interest**

The authors declare no conflict of interest.

#### References

[1] Ogunkunle, O., Ahmed, N.A., 2021. Overview of biodiesel combustion in mitigating the adverse impacts of engine emissions on the sustainable human-environment scenario. Sustainability. 13(10).

- [2] Skrúcaný, T., Kendra, M., Stopka, O., et al., 2019. Impact of the electric mobility implementation on the greenhouse gases production in Central European countries. Sustainability. 11(18).
- [3] Raj, F.I., Appadurai, M., 2021. The hybrid electric vehicle (HEV)—an overview. In: Emerging Solutions for e-Mobility and Smart Grids: Select Proceedings of ICRES 2020. Springer: Singapore. pp. 25–36.
- [4] Zhang, B., Maloney, D., Harun, N.F., et al., 2022. Rapid load transition for integrated solid oxide fuel cell–Gas turbine (SOFC-GT) energy systems: A demonstration of the potential for grid response. Energy Conversion and Management. 258, 115544.
- [5] Kazula, S., De Graaf, S., Enghardt, L., 2022. Preliminary safety assessment of PEM fuel cell systems for electrified propulsion systems in commercial aviation. In Proceedings of the 32nd European Safety and Reliability Conference (ESREL 2022), Dublin, Ireland, August 28–September 1, 2022; pp. 1–8.
- [6] Chen, Y., Wang, N., 2019. Cuckoo search algorithm with explosion operator for modeling proton exchange membrane fuel cells. International Journal of Hydrogen Energy. 44(5), 3075–3087.
- [7] Malik, F.R., Zhang, T., Kim, Y.B., 2020. Temperature and hydrogen flow rate controls of diesel autothermal reformer for 3.6 kW PEM fuel cell system with autoignition delay time analysis. International Journal of Hydrogen Energy. 45(53), 29345–29355.
- [8] Brezak, D., Kovač, A., Firak, M., 2023. MAT-LAB/Simulink simulation of low-pressure PEM electrolyzer stack. International Journal of Hydrogen Energy. 48(16), 6158–6173.
- [9] Lv, X., Guo, X.Y., Zhou, H.L., et al., 2023. Modeling & dynamic simulation of high-power proton exchange membrane fuel cell systems. In Proceedings of the 8th Asia Conference on Power and Electrical Engineering (ACPEE), Tokyo, Japan, 14–16 April 2023; pp. 1206–1212.
- [10] Subedi, A., Thapa, B.S., 2022. Parametric modeling of re-electrification by green hydrogen as an alternative to backup power. IOP Conference Series: Earth and Environmental Science. 1037, 012057.
- [11] Sharma, A., 2021. Improvement in the performance of proton exchange membrane fuel cell with effects of the thickness and conductivity of the membrane. International Research Journal of Engineering and Technology. 8(3).
- [12] Gadducci, E., Lamberti, T., Bellotti, D., et al., 2021. BoP incidence on a 240 kW PEMFC system in a ship-like environment, employing a dedicated fuel cell stack model. International Journal of Hydrogen Energy. 46(47), 24305–24317.

- [13] Chen, M., Al-Subhi, K., Al-Rajhi, A., et al., 2023. Numerical evaluation of hydrogen production by steam reforming of natural gas. Advances in Geo-Energy Research. 7(3), 141–151.
- [14] Corrêa, J.M., Farret, F.A., Canna, L.N., 2001. An analysis of the dynamic performance of proton exchange membrane fuel cells using an electromechanical model. In Proceedings of the IEEE IECON'01 Conference, Denver, CO, USA, November 29–December 2, 2001; pp. 141–146.
- [15] Mann, R.F., Amphlett, J.C., Hooper, M.A.I., et al., 2000. Development and application of a generalised steady-state electrochemical model for a PEM fuel cell. Journal of Power Sources. 86, 173–180.
- [16] Khadhraoui, A., Selmi, T., Cherif, A., et al., 2019. A theoretical study on the simultaneous hydrogen production and consumption in proton exchange membrane fuel cell/battery electric vehicles. International Journal of Membrane Science and Technology. 9(2).
- [17] Yu, D., Yuvarajan, S., 2005. Electronic circuit model for proton exchange membrane fuel cells. Journal of Power Sources.142(1–2), 238–242.
- [18] Ramezani, M., Chitsazan, S., Pouria, A., 2021. Performance analysis of a degraded PEM fuel cell stack for hydrogen passenger vehicles based on machine learning algorithms in real driving conditions. Energy Conversion and Management. 248, 114793.
- [19] Amrouche, F., Mahmah, B., Belhamel, M., et al., 2005. Modélisation d'une pile à combustible PEMFC alimentée directement en hydrogène-oxygène et validation expérimentale. Renewable Energy Review. 8, 109–121.
- [20] Maher, A.R., Al-Baghdadi, S., 2005. Modelling of proton exchange membrane fuel cell performance based on semi-empirical equations. Renewable Energy. 30, 1587–1599.
- [21] Fowler, M.W., Mann, R.F., Amphlett, J.C., et al., 2002. Incorporation of voltage degradation into a generalised steady state electrochemical model for a PEM fuel cell. Journal of Power Sources. 106, 274–283.
- [22] Saleh, Z.H., 2016. Simplified mathematical model of proton exchange membrane fuel cell based on horizon fuel cell stack. Journal of Modern Power Systems and Clean Energy. 4, 668–679.
- [23] Corrêa, J.M., Farret, F.A., Gomes, J.R., et al., 2003. Simulation of fuel-cell stacks using a computercontrolled power rectifier with the purposes of actual high-power injection applications. IEEE Transactions on Industry Applications. 39(4), 1136– 1142.
- [24] Çeven, S., Albayrak, A., Bayır, R., 2020. Real-time range estimation in electric vehicles using fuzzy logic classifier. Computers and Electrical Engineer-

- ing. 83, 106580.
- [25] Selmi, T., Khadhraoui, A., Cherif, A., 2022. Fuel cell-based electric vehicles technologies and challenges. Environmental Science and Pollution Research. 29(52), 78121-78131.
- Proton exchange membrane fuel cells: Advances and challenges. Polymers. 13(18), 3064.
- [27] Pourrahmani, H., Yavarinasab, A., Siavashi, M., et
- al., 2022. Progress in the proton exchange membrane fuel cells (PEMFCs) water/thermal management: From theory to the current challenges and real-time fault diagnosis methods. Energy Reviews. 1(1), 100002.
- [26] Cruz, T.M., Escorihuela, J., Solorza-Feria, O., 2021. [28] Butt, H.A., 2023. Electric vehicles and performance indicators: Sustainability analysis for the city of Turin [PhD dissertation]. Politecnico di Torino: Turin, Italy.